Bond University

Research Repository

Improving Hilbert–Huang transform for energy-correlation fluctuation in hydraulic engineering

Lu, Shibao; Zhang, Xiaoling; Shang, Yizi; Li, Wei; Skitmore, Martin; Jiang, Shuli; Xue, Yangang

Published in:
Energy

DOI:
10.1016/j.energy.2018.08.088

Licence:
CC BY-NC-ND

Link to output in Bond University research repository.

Recommended citation(APA):
Lu, S., Zhang, X., Shang, Y., Li, W., Skitmore, M., Jiang, S., & Xue, Y. (2018). Improving Hilbert–Huang transform for energy-correlation fluctuation in hydraulic engineering. *Energy*, *164*, 1341-1350. https://doi.org/10.1016/j.energy.2018.08.088

General rights
Copyright and moral rights for the publications made accessible in the public portal are retained by the authors and/or other copyright owners and it is a condition of accessing publications that users recognise and abide by the legal requirements associated with these rights.

For more information, or if you believe that this document breaches copyright, please contact the Bond University research repository coordinator.

Download date: 19 May 2024

Improving Hilbert–Huang Transform for Energy-Correlation Fluctuation in Hydraulic Engineering

Shibao Lu[1], Xiaoling Zhang[2], Yizi Shang[3]*, Wei Li[1], Martin Skitmore[4], Shuli Jiang[1], Yangang Xue[5]

[1] School of Public Administration, Zhejiang University of Finance and Economics, Hang Zhou 310018, China;
[2]Department of Public Policy, City University of Hong Kong, Hong Kong
[3] School of Chemical Science and Engineering, KTH - Royal Institute of Technology, Teknikringen 42, 114 28 Stockholm;
[4] School of Civil Engineering and Built Environment, Queensland University of Technology (QUT), Brisbane 4001, Australia;
[5] LanZhou Institute of Technology, Lanzhou 730000, China.
***Corresponding author：** E-mail: address:xiaoling.zhang@cityu.edu.hk , **yzshang@foxmail.com**

Abstract: Intense vibrations in hydraulic turbine generator unit draft tubes lead to a run-out of the unit shafting and threaten its safe and stable operation. Correct maintenance is therefore important for the safe operation of such units. This study involves assessing the condition of the turbine generator unit by extracting the feature information of its vibration signals. Based on previous research, we present an enhanced Hilbert–Huang transform (HHT) method with an energy-correlation fluctuation criterion to extract feature information and effectively verify the method with simulated signals. An inspection application based on the signal from a vortex strip in the draft tube of a prototype turbine under suboptimal operating conditions indicates that this method is more effective than the traditional one, with a better component identification capability and better suited to the analysis of the complex and dynamic feature information of hydro turbines.

Keywords: Condition-based maintenance; Hilbert–Huang transform method; vortex strip in draft tube; dynamic feature information; false component

1. Introduction

The corrective maintenance of hydraulic turbine generator units is very important, as serious damage leads to the run-out of shafting, undermining their safe and stable operation. One form of corrective maintenance is condition-based maintenance (CBM). This tracks the operating conditions and variations in the unit's performance to identify and locate problems in time to prevent damage from deterioration. This involves accurately assessing the operating condition of a unit in its operating environment to determine the time, content, and method of maintenance needed, and to predict its remaining service life [1]. For hydraulic generator units, it is important to extract signal feature information from the vortex strip in the draft tube, as this improves the capability of CBM in monitoring, diagnosis, and analysis of equipment [2,3].

A hydroelectric generating unit is a complex nonlinear power system. The development and emergence of operational process faults entail a large number of uncertainties. However, the traditional fault diagnosis modeling theory and method cannot easily and accurately describe a large number of uncertainty factors, due to the fault feature acquisition of the hydroelectric generating unit power system [4]. It is difficult to obtain an accurate diagnosis of the actual conditional maintenance system of a hydroelectric generating unit, which greatly restricts application of the theory and method of hydroelectric generating unit state-based maintenance in engineering practice. The working medium of the hydroelectric generating unit, a special rotating machine, is water. Due to the uniqueness of its operating conditions, the vibration characteristics of the hydroelectric generating unit are quite different to those of general power machinery [5], as

the cause of the vibration is much more complicated. In particular, the spindle system, which is an important part of the hydroelectric generating unit, has a complex structure. When it is defectively designed, manufactured or installed, or excited under certain external loads, it will exhibit complex vibrational phenomena.

In the past, the measurement of the vibration of the unit was based on a general study of the vibration of the entire unit. However, the characteristics of the unit vibration caused by different vibration sources vary, and mainly reflect the frequency band distribution of the frequency signal [6,7]. Each type of vibration signal has its own characteristic frequency. The amount of data to be screened out for feature judgment is very large, and no quick and accurate diagnosis results can be obtained. It should be noted that the vibration caused by the operation of the unit is often the main factor affecting the stability of the entire unit [8,9]. Therefore, when studying the vibration of the unit, it is necessary to identify the main factors causing the vibration, extract the characteristics, and accurately determine the fault point in time according to the vibration characteristics to guarantee the unit's safe operation.

The HHT is a new type of signal transform method that involves decomposing signals into several intrinsic mode functions (IMFs) by empirical mode decomposition (EMD), and then solves the instantaneous frequency of each IMF by Hilbert transform to analyze the non-linear and non-stationary signals.

HHT is composed of empirical mode decomposition and the corresponding Hilbert transform. Its basic idea is that the original signal is decomposed into a series of combinations, called IMFs, where the meaningful instantaneous frequency and instantaneous amplitude are defined and

calculated with the analytic signal phase, and the Hilbert time-frequency spectrum (HHS) of the signal is obtained.

This method has aroused great interest among science researchers and has been successfully used in a variety of fields. Compared with the traditional time-frequency analysis method, the EMD method has many advantageous characteristics, the most typical ones being adaptivity, completeness, and orthogonality. Mohammadilandi et al. [8] adopted the HHT time-frequency analysis method as part of an EMD using the Hilbert transform to obtain instantaneous frequencies. First, the Hilbert transform was applied to the IMFs in order to reconstitute and analyze the signal; then the analytical signals were parsed to obtain the instantaneous frequency of the derivative at different phases of the analytical signal. For such instantaneous frequency methods used in finding vibration signal problems, especially where frequency-modulated (FM) and amplitude-modulated (AM) signals are concerned, the instantaneous frequency obtained will have relatively large deviations. Sometimes, negative frequencies may even occur. This kind of instantaneous frequency is difficult to explain and does not have any real physical significance. Lu [3] adopted an EMD and AR (auto-regression) model to extract dynamic characteristic information from draft tube pressure fluctuations, the EMD adaptively decomposing the signal into IMFs. This decomposition method has no restrictions where flat time-frequency representations are concerned, and therefore each IMF reflects a special type of signal frequency information. The basis function of the EMD method, which is a series of sine waves having variable amplitude and an adjustable frequency, is obtained adaptively according to the signal characteristics during the decomposition, and represents the nonlinearity and non-stationarity of the signal.

After many years of field testing the EMD method [10-11], the author discovered that the shape of its time series had a relatively specific and abnormal waveform when a fault occurred, with its periodicity presented repeatedly. This waveform reflects the fault characteristics; however, a mathematical model reflecting the morphology would be required for describing the waveform characteristic of a time series.

However, some state or output signals of the system can be measured during this process. Because the characteristic signals can be easily obtained, signal-processing techniques provide an effective way to solve such problems. Therefore, finding an appropriate signal analysis and processing method, exploring weak fault signal detection, non-stationary signal extraction, and analysis technology, and expanding the intelligent fault diagnosis model of hydraulic turbines, have all become important parts of this study [12–14]. Ahmetović et al. [9] overcomes this to some extent by offering an improved HHT method based on energy-correlation fluctuation. Our paper develops this further by first addressing the problem of the *false component* in HHT by goodness-of-fit testing based on HHT theory. This identifies and eliminates the false component based on the similarity of the IMF and the original signal after decomposition. A simple and efficient method is developed to eliminate the false component, which is illustrated in an analysis of the shafting signal of a prototype turbine in suboptimal operating conditions. This demonstrates that the method is able to properly eliminate the false component and extract the true dynamic feature information from the turbine, proving this method much more advantageous and rational than the traditional method.

2. Primary algorithm for the HHT

A hydro turbine generator unit in operation is under the influence of hydraulic power, machine power, and electromagnetism, and therefore hydraulic turbine signals are usually neither linear nor stationary [15,16]. An analysis method based on HHT is not only high-resolution in the time and frequency domains, but it also self-adaptively decomposes signals into different scales, and extracts dynamic feature information from the turbine by Hilbert spectrum analysis.

The core of HHT involves obtaining a series of IMFs by the EMD of signals to shape the IMF as a narrow band and stationary signal. The IMF components must meet the following two conditions [17–19]: ① there can be only one point of difference between the extreme points and crossover points of the component signal; and ② the mean value at any point of the upper and lower envelope curves must be zero.

The EMD algorithm extracts the IMFs based on the local feature time scale of the signal, and the signal stationary processing generates a data sequence under different scales. The algorithm process is as follows [20,21]: ① determine local maximum sequence $x_{\max}$ and local minimum sequence $x_{\min}$; ② determine the upper and lower envelopes and local mean value $m(t) = (x_{\max} + x_{\min})/2$ of signal $x(t)$ according to $x_{\max}$ and $x_{\min}$; ③determine the difference between the signal and the local mean: $h_1(t) = x(t) - m(t)$; ④ because an asymmetric wave exists in a nonlinear and non-stationary signal, $m(t)$ is not the true local mean. Therefore, $x(t)$ is replaced with $h_1(t)$, and the above three steps are repeated until h_{1k} meets the basic condition of the IMF. Suppose $c_1 = h_{1k}$ and $r_1 = x(t) - c_1$, then

$$x(t) = \sum_{i=1}^{n} c_i(t) + r_n(t) \tag{1}$$

where $c_i(t)$ is the IMF obtained by EMD, and $r_n(t)$ is a trend remainder term of the signal. After obtaining the analytic signal by Hilbert transform, the instantaneous frequency $w_i(t)$ and instantaneous amplitude $a_i(t)$ can be found. Indicate $a_i(t)$ on the time-frequency joint plane to obtain the Hilbert amplitude spectrum of $c_i(t)$:

$$H_i(w,t) = \begin{cases} 0, w \neq w_i(t) \\ a_i(t), w = w_i(t) \end{cases} \tag{2}$$

Then, ignore the remainder term $r_n(n)$ to obtain the Hilbert spectrum of the signal:

$$H(w,t) = \mathrm{Re}\sum_{i=1}^{n} a_i(t) e^{j\int w_i(t)dt} \tag{3}$$

3. Improved HHT

The EMD process involves obtaining the IMF of the signal component, namely the IMF component is orthogonal. However, the algorithm is unable to ensure the orthogonality of the IMF in the actual decomposition, and the number of components is dependent on extreme orders, without taking into consideration the influence of the sampling interval and noise on the decomposition. In order to obtain the real component of the IMF, Huang [1] proposed an index of orthogonality (IO). Suppose the IO value of any two components of the IMF is no more than 0.1 and almost 95% of the values are distributed within the range of two standard deviations of the mean value. If the IMF is subject to a single statistical analysis, then the value of the IO is restricted to an interval of 0.05.

Moreover, only a few signals meet this supposition: some components of the IMF generate a false composition after decomposition due to “flying wing” on the endpoints. Because the IMF components are in an array from high to low in terms of local instantaneous frequency, the IMF components obtained attenuate in terms of amplitude and frequency, with energy degradation (in

inches) showing an apparent declining trend [20,21]. Therefore, the energy-correlation fluctuation method of Xue et al. [15,16] was extended to find the difference between the IMF components and the original signal to determine and identify false IMF components. The algorithm process is as follows:

$$\varepsilon_i = \frac{E_{imfi}}{E_x} = \frac{\int_0^T \left| imf_i(t) \right|^2 dt}{\int_0^T \left| x(t) \right|^2 dt} \tag{4}$$

where E_{imfi} indicates the energy of the IMF component, E_x is the energy of the original signal, and ε_i is the specific value of the two, indicating the energy fluctuation of the IMF component.

In engineering practice, the signal is discrete after sampling, so (4) is transformed into

$$\varepsilon_i = \frac{\sum_{j=1}^{n} \left| (imf_i(j) - \overline{imf_i(j)}) \right|^2}{\sum_{j=1}^{n} \left| (x(j) - \overline{x(j)}) \right|^2} \tag{5}$$

where $\overline{imf_j}$ and $\overline{x(j)}$ are mean values of the IMF components and original signals respectively, being the statistical parameters for the measurement of random signals.

Energy is a feature parameter of the signal [24]. The energy fluctuation method monitors the energy fluctuation between the IMF component and original signal after decomposition to select the component and set the feature to identify the false component in the above-mentioned energy-correlation fluctuation method.

In addition, information useful for indicating the turbine operating condition from its signal often exists in the low frequency zone and low energy component signal, showing that identifying a false component by energy fluctuation is only partly adequate. Because correlation describes the similarity and internal connection between two signals [25], the real IMF component and the original signal after EMD are closely correlated. Accordingly, the correlation between the IMF

component and the turbine shafting signals is used to identify the false component, namely the correlation fluctuation ratio

$$\rho_i = \frac{C_{x(t)imfi(t)}}{\sigma_{x(t)}\sigma_{imfi(t)}} \tag{6}$$

where the numerator is the correlation coefficient between the IMF component and the original signal, which describes the similarity between the two signals, the denominator is the standard deviation of the difference between the original signal and the IMF component, and their ratio is the correlation fluctuation ratio ρ_i.

Identification condition 1: The IMF component with the higher correlation fluctuation ratio ρ_i is the real component containing the turbine's operating condition. If the correlation fluctuation ratio ρ_i is smaller than the 0.05 threshold value and fails to meet identification condition 1, then the component is deemed a false IMF component.

(Insert Fig.1 here)

Identification condition 2: This restricts the IO to an interval of 0.05; therefore, the energy fluctuation method is able to reveal the intrinsic relationship between the IMF component and the original signal to meet the requirement of orthogonality to obtain the real IMF component with high computational efficiency.

After selection, the so-called false IMF component is not simply eliminated. Instead, the component and trend terms are totaled to obtain a new trend remainder term. Fig. 1 shows the simulated signal waveform and result after EMD, with the amplitude and frequency subjected to modulation. The simulated signal contains only two feature frequency components, while Fig. 1(b) shows three IMF components and one trend term after EMD. Obviously, there is a "flying wing" at the endpoints in the decomposition, due to the generation of a false component.

Adopting the energy-correlation fluctuation method to track the EMD process involves selecting a real IMF component and eliminating false components [26]. During selection, the energy-correlation fluctuation ratio between the IMF component and the analytical signal is as shown in Fig. 2. This shows that, although the three IMF components obtained in the standard EMD meet identification condition 1 for the energy-correlation fluctuation method, only the first two components meet identification condition 2; the third component fails to meet the condition. Therefore, the component is false and needs to be eliminated.

(Insert Fig.2 here)

To reveal the variation further before and after signal decomposition, the energy-correlation fluctuation method uses parameterization to eliminate false components, the result of which is shown in Table 1.

(Insert Table.1 here)

E_x in Table 1 is the total energy of the simulated signal, E_{x1} and E_{x2} are the component and energy respectively at the two frequencies, $E_{x'}$ is the total energy of the signal after decomposition, while E_{imf1}, E_{imf2}, and E_{imf3} are the energies of the three IMF components after decomposition. This results in six fluctuation ratios, namely $\varepsilon_1, \varepsilon_2, \varepsilon_3$, and ρ_1, ρ_2, ρ_3.

As Table 1 indicates, the total energy of the simulated signal before and after decomposition remains almost one of conservation, and complies with the completeness and orthogonality of the EMD [27,28]. With the energy-correlation fluctuation method, the correlation fluctuation ratio ρ_3 of the third IMF component is far smaller than 0.05. Therefore, the component is a false IMF component to be eliminated before the Hilbert transform. That is, the trend of the false component and original term need to be totaled to form a new trend remainder term. After improvement, the

IMF component and the trend remainder term are as shown in Fig. 3. After elimination of the false component, the simulated signal has an *IO* of 0.0148. Before improvement, its *IO* was 0.0195, which is 24.1% higher. The improved IMF component was subjected to the Hilbert transform to obtain Fig. 4, this being the Hilbert spectrum of the simulated signal:

(Insert Fig.3 here)

(Insert Fig.4 here)

4. Dynamic feature information extraction from a prototype turbine using the improved HHT

4.1 General situation of unit and test

A hydro turbine under suboptimal operating conditions generates various vibration phenomena, including a great number of dynamic features. Research into transient vibration under suboptimal operating conditions is therefore significant for the design, operation, and maintenance of hydro turbines [29]. In order to eliminate irrelevant component interference, the energy-correlation fluctuation method was applied to the No. 1 hydraulic turbine of the Tagake Hydraulic Power Plant in Xinjiang for prototype testing. The types of generator units in the power plant were HLA801-LJ-215 and SF24.5-20/4250; the turbine had a nominal speed of 300 r/min (5 Hz), a nominal power of 24.5 MW, and a 74 m operating head. The measured signal was obtained from a turbine with an output of 40-55% and nominal capacity of 10 MW-14 MW in operating conditions. The sampling frequency was 200 Hz and the data length was 1000. There was also a vortex sensor on the upper guide bearing, lower guide bearing, and turbine guide bearing along a $+X/-Y$ direction, respectively, to measure the maximum shaft run-out. The vortex sensor for measurement of the run-out phase was installed on a turbine guide bearing in the $-Y$ direction,

the measuring point for vertical and horizontal vibration was prepared on the upper generator bracket in the $+Y$ direction, and the measuring point for horizontal vibration was prepared on the lower generator bracket in the $+Y$ direction. A measuring point was also prepared on the top cover (turbine guide oil basin cover) in the $-Y$ direction.

4.2 Dynamic feature information extraction

A shafting run-out analysis as shown in Fig. 5 was used to monitor the turbine under operating conditions for a low frequency pulse because of the vortex strip in the draft tube. This involves adopting an EMD to decompose the run-out signal, as shown in Fig. 6, to obtain the features of frequency and amplitude modulation apparent in the first five of seven IMF components.

(Insert Fig.5 here)

(Insert Fig6. here)

Because hydro turbines have complex internal flow conditions under suboptimal operating conditions, and generate various vibration signals, the IMF components obtained by decomposition were subjected to the Hilbert spectrum analysis as shown in Fig. 7. This shows the turbine's speed of 5 Hz to be the leading component, containing some low frequency components and high frequency components of 50 Hz. The spectrum is cluttered, with parent aliasing and distortion in the low frequency zones after preliminary determination. The shafting signal generates a false component in decomposition, resulting in aliasing with the low frequency signals [30].

(Insert Fig.7 here)

Adopting the energy-correlation fluctuation method allows the identification of false IMF components and calculation of fluctuation ratios to obtain Fig. 8. From this, it is clear that the first two IMF components fail to meet identification condition 1, namely, the components decline in energy, and two are suspected of being false components. In addition, the second and seventh IMF components fail to meet identification condition 2. After a comprehensive analysis, the second and seventh IMF components were identified as the components to be eliminated. The first IMF was then subjected to individual extraction and analysis, producing a Hilbert spectrum as shown in Fig. 9.

(Insert Figure 8 here)

(Insert Figure 9 here)

From the field test, and from knowing the typical faults of hydraulic turbines, the IMF component analysis shows that the 50 Hz frequency is a result of the monitoring system being interfered with by an imperfect earth in the power plant. The parameterization analysis is shown in Table 2, where $E_{imf\,1}$ - $E_{imf\,7}$ denotes the energy of the seven IMF components after decomposition, together with the calculated ε_1 - ε_7 and ρ_1 - ρ_7 energy-correlation fluctuation ratios.

(Insert Table 2 here)

This shows that the energy-correlation fluctuation method necessitates the mutual verification of two conditions in identifying the false component and drawing the correct conclusion.

Fig. 10 shows the Hilbert spectrum of the shafting run-out signal of the turbine after elimination of IMF components 1, 2, and 7. This shows that the shafting run-out response contains a speed frequency and low frequency component of 2.4 Hz, of which the leading component has a speed frequency of 5 Hz. In theory, mechanical factors should have little effect on the vibration of

a well-maintained generator unit, as its vibration should be mainly due to hydraulic factors. When a mixed-flow turbine has an extremely suboptimal design, the rotational velocity component at the outlet of the turbine runner generates an unstable vortex strip in the draft tube that leads to pressure pulsation, with a pulse frequency of around 1/2–1/5 of the speed frequency of the turbine [31,32].

Field observations indicate that the turbine draft tube has a serious vortex strip in such suboptimal operating conditions. Therefore, according to the above-mentioned turbine vibration mechanism [33–35], the low frequency component in the spectrum is higher in energy, with the frequency range being the shafting run-out frequency due to the low frequency vortex strip of the draft tube. Both theory and test analyses indicate that the shafting run-out signal contains not only a speed frequency component but also a shafting run-out component due to the low frequency vortex strip. The two results are in full accord, demonstrating that the improved HHT method is better for analyzing turbine-shafting signals.

(Insert Fig. 10 here)

(Insert Fig. 11 here)

Fig. 11 shows the Hilbert boundary spectrum of the signal before and after improvement, in which the red solid line is the boundary spectrum of the signal after improvement, and the blue dotted line is the boundary spectrum before improvement. The three marked areas from right to left are the IMF1, IMF2, and IMF7 false components, respectively. Except for the frequency spectrum zone of the false components, the two curves largely coincide. That is, the entire trend and real signal information remain unchanged, showing an apparent speed frequency component and a low frequency vortex strip component.

In order to verify the method further in terms of its effectiveness and accuracy, a basic frequency of the low frequency vortex strip in the draft tube was determined to be 2.45 Hz, with the frequency being the actual feature frequency of the low frequency vortex strip. Before improvement, it was difficult to determine whether there was a low frequency vortex strip and feature frequency due to false component interference. After improvement, the feature frequency of the shafting vortex strip was smaller than the actual value, mainly due to transfer function attenuation of the sensor in the monitoring process, but with an influence of only 2.04%.

5. Conclusions

(1) An improved Hilbert–Huang transform method based on energy-correlation fluctuation modification was presented to solve the false component problem in hydro turbine fault detection [36]. The improved method was applied to a prototype turbine under suboptimal operating conditions to show that, from dynamic signal feature extraction of the shafting, the run-out response in the operating condition was mainly composed of a speed frequency and low frequency component of 2.4 Hz. The leading component was a speed frequency of 5 Hz when compared with the HHT method before improvement, which indicated that the improved HHT method obtained a better result, having the advantage of greater accuracy and stability.

(2) The energy-correlation fluctuation method was free from aliasing and distortion due to the false component identification and instantaneous frequency estimation capabilities of the IMF in EMD, ensuring a higher time frequency resolution of the Hilbert spectrum and greater suitability to the analysis of complex and dynamic turbine feature information.

(3) An inspection application based on the signal from the vortex strip in the draft tube of a prototype turbine under suboptimal operating condition indicated that the energy correlation

fluctuation method was more effective than the traditional one. After improvement, the feature frequency of the shafting vortex strip was smaller than the actual value, mainly due to transfer function attenuation of the sensor in the monitoring process, but with an influence of only 2.04%.

6. Conflict of Interest

The authors declare they have no conflict of interest in this work.

7. Acknowledgments

This research was funded by the National Natural Science Foundation of China (Grant Nos 51379219 and 51769012), Zhejiang Province Funds for Distinguished Young Scientists (Grant No. LR15E090002), and Gansu Province Natural Science Foundation of China (Grant No. 1506RJZA059). The work described in this paper was also substantially supported by the grant from the Research Grants Council of the Hong Kong Special Administrative Region, China (Project No. CityU 11271716 and CityU 21209715).

References

[1] Huang N E, Shen Z, Long S R. A new view of nonlinear water waves: the Hilbert spectrum[J]. Annual review of fluid mechanics, 1999, 31(1): 417-457.

[2] Huang, N. E., Wu, M. L. C., Long, S. R., Shen, S. S., Qu, W., Gloersen, P., Fan, K. L. (2003, September). A confidence limit for the empirical mode decomposition and Hilbert spectral analysis. In *Proceedings of the royal society of london a: Mathematical, physical and engineering sciences* (Vol. 459, No. 2037, pp. 2317-2345). The Royal Society.

[3] Lu S, Wang J, Xue Y. Study on multi-fractal fault diagnosis based on EMD fusion in hydraulic engineering[J]. Applied Thermal Engineering, 2016, 103: 798-806.

[4] Peng Z K, Peter W T, Chu F L. An improved Hilbert–Huang transform and its application in vibration signal analysis[J]. Journal of sound and vibration, 2005, 286(1-2): 187-205.

[5] Chen Y, Lan L. Fault detection, diagnosis and data recovery for a real building heating/cooling billing system[J]. Energy Conversion and Management, 2010, 51(5): 1015-1024.

[6] Lu S, Wang J, Shang Y, Bao, H., Chen, H. Potential assessment of optimizing energy structure in the city of carbon intensity target[J]. Applied energy, 2017, 194: 765-773.

[7] Shang Y, Lu S, Li X, Hei, P., Lei, X., Gong, J., ... & Wang, H. Balancing development of major coal bases with available water resources in China through 2020[J]. Applied energy, 2017, 194: 735-750.

[8] Mohammadilandi, M., Mohammadi, M., Rastegar, M. Simultaneous determination of optimal capacity and charging profile of plug-in electric vehicle parking lots in distribution systems, Energy, 2018:158:504-511.

[9] Ahmetović, E., Ibrić, N., Kravanja, Z., Grossmann, I. E., Maréchal, F., Čuček, L., & Kermani, M. Simultaneous optimisation and heat integration of evaporation systems including mechanical vapour recompression and background process. Energy, 2018, 158:1160-1191.

[10] Deering R, Kaiser J F. The use of a masking signal to improve empirical mode decomposition. IEEE International Conference on Acoustics. Speech and Signal Processing 2005, 7(4): 485-488.

[11] Wang, S., Yu, L., Tang, L., Wang, S. A novel seasonal decomposition based least squares support vector regression ensemble learning approach for hydropower consumption forecasting in China. Energy, 2011, 36(11): 6542-6554.

[12] Zhu, Y., Zhang, Y., Lu, L. Influence of crystallization temperature on ionic conductivity of lithium aluminum germanium phosphate glass-ceramic. Journal of Power Sources, 2015, 290: 123-129.

[13] Dätig M, Schlurmann T. Performance and limitations of the Hilbert–Huang transformation (HHT) with an application to irregular water waves. Ocean Engineering, 2004, 31(14-15): 1783-1834.

[14] Brkovic, A., Gajic, D., Gligorijevic, J., Savic-Gajic, I., Georgieva, O., Di Gennaro, S. Early fault detection and diagnosis in bearings for more efficient operation of rotating machinery. Energy, 2017, 136: 63-71.

[15] Rivarolo, M., Bellotti, D., Mendieta, A., Massardo, A. F. Hydro-methane and methanol combined production from hydroelectricity and biomass: Thermo-economic analysis in Paraguay. Energy Conversion and Management, 2014, 79(3): 74-84.

[16] Huang, S. R., Ma, Y. H., Chen, C. F., Seki, K., Aso, T. Theoretical and conditional monitoring of a small three-bladed vertical-axis micro-hydro turbine. Energy Conversion and Management, 2014, 86(10): 727-734.

[17] Fan, Y., Mu, A., Ma, T. Modeling and control of a hybrid wind-tidal turbine with hydraulic accumulator. Energy, 2016, 112: 188-199.

[18] Peng, Z. K., Peter, W. T., Chu, F. L. An improved Hilbert-Huang transform and its application in vibration signal analysis. Journal of Sound and Vibration, 2005, 286(1-2): 187-205.

[19] Peng, Z. K., Peter, W. T., Chu, F. L. A comparison study of improved Hilbert-Huang transform and wavelet transform: Application to fault diagnosis for rolling bearing. Mechanical Systems and Signal Processing, 2005, 19(5):974-988.

[20] Yinfeng, D., Yingmin, L., Mingkui, X., Ming, L. Analysis of earthquake ground motions using an improved Hilbert-Huang transform. Soil Dynamics and Earthquake Engineering, 2008, 28(1):7-19.

[21] Qin, S. R., Zhong, Y. M. New envelope algorithm of Hilbert-Huang transform. Mechanical Systems and Signal Processing, 2006, 20(8):1941-1952.

[22] Pires, V. F., Martins, J. F., Pires, A. J. Eigenvector/eigenvalue analysis of a 3D current referential fault detection and diagnosis of an induction motor. Energy Conversion and Management, 2010, 51(5): 901-907.

[23] Lin, L., Hongbing, J. Signal feature extraction based on an improved EMD method Measurement, 2009, 42(5): 796-803.

[24] Xie, H., Wang, Z. Mean frequency derived via Hilbert-Huang transform with application to fatigue EMG signal analysis. Computer Methods & Programs in Biomedicine, 2006, 82(2): 114-120.

[25] Wang T, Zhang M, Yu Q, Zhang H. Comparing the applications of EMD and EEMD on time–frequency analysis of seismic signal. Journal of Applied Geophysics, 2012, 83(8): 29-34.

[26] Yu D, Yang Y, Cheng J. Application of time–frequency entropy method based on Hilbert–Huang transform to gear fault diagnosis. Measurement, 2007, 40(9-10): 823-830.

[27] Kim D, Paek S-H, Oh H-S. A Hilbert–Huang transform approach for predicting cyber-attacks. Journal of the Korean Statistical Society, 2008, 37(3): 277-283.

[28] Lu S, Zhang X, Bao H, Skitmore, M. Review of social water cycle research in a changing environment. Renewable and Sustainable Energy Reviews, 2016, 63: 132-140.

[29] Pigorini, A., Casali, A. G., Casarotto, S., Ferrarelli, F., Baselli, G., Mariotti, M., ... & Rosanova, M. Time–frequency spectral analysis of TMS-evoked EEG oscillations by means of Hilbert–Huang transform. Journal of Neuroscience Methods, 2011, 198(2): 236-245.

[30] Lang, Z. Q., Peng, Z. K. A novel approach for nonlinearity detection in vibrating systems. Journal of Sound and Vibration, 2008, 314(3-5): 603-615.

[31] Liu, H., Abraham, A., Clerc, M. Chaotic dynamic characteristics in swarm intelligence. Applied Soft Computing, 2007, 7(3): 1019-1026.

[32] Cai, J. A combinatorial filtering method for magnetotelluric time-series based on Hilbert–Huang transform. Exploration Geophysics, 2013, 45(2): 63-73.

[33] Yang, X. L., Yan, H., Xu, Z., Ren, Z. R., Song, J. Z., Yao, Y. H., Li, Y. J. ECG de-noising based on Hilbert–Huang transform. Acta Electronica Sinica, 2011, 39: 819–824.

[34] He, K., Yu, L., Tang, L. Electricity price forecasting with a BED (Bivariate EMD Denoising) methodology. Energy, 2015, 91: 601-609.

[35] An, X., Jiang, D., Li, S., Zhao, M. Application of the ensemble empirical mode decomposition and Hilbert transform to pedestal looseness study of direct-drive wind turbine. Energy, 2011, 36: 5508-5520.

[36] Lu, S., Wei, J., Bao, H., Xue, Y., Ye, W. The dynamic hydropower troubleshooting information based on EMD multi-scale feature entropy extraction. International Journal of Mobile Communications, 2017, 15(6): 677-692.

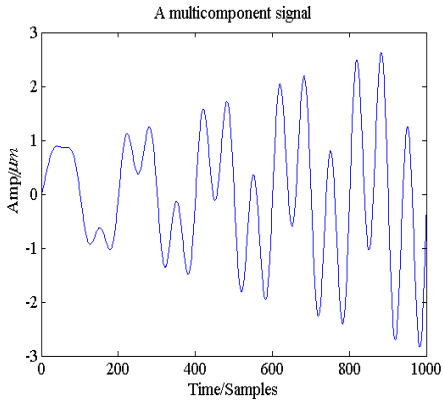

(a) Simulated signal

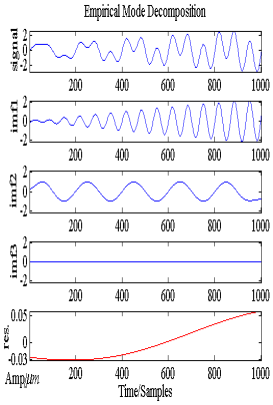

(b) **Signal EMD**

Fig .1 Simulate Signal and result of EMD

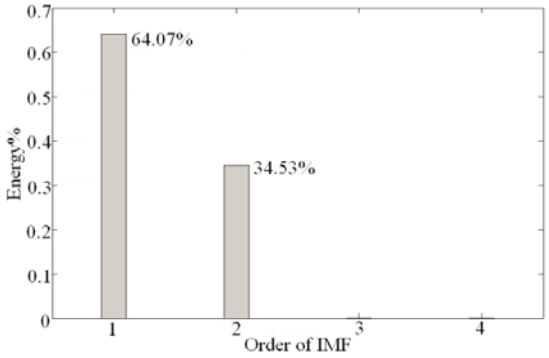

(a) Energy fluctuation ratio

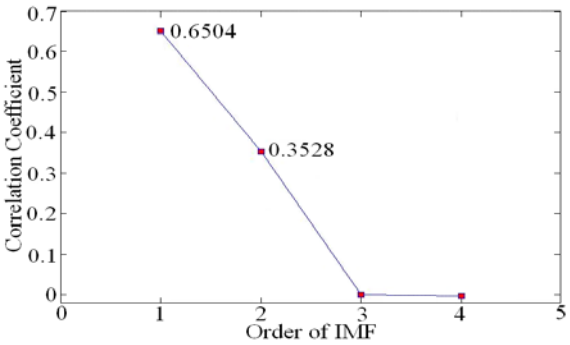

(b) Correlation fluctuation ratio

Fig .2 Energy-Correlation Fluctuation

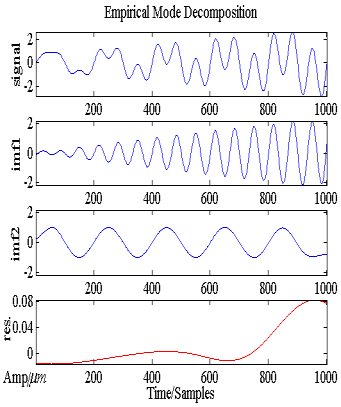

Fig .3 Improved IMF Components

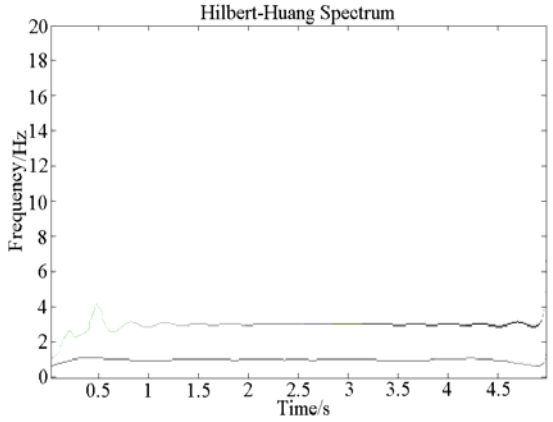

Fig .4 Improved HHS

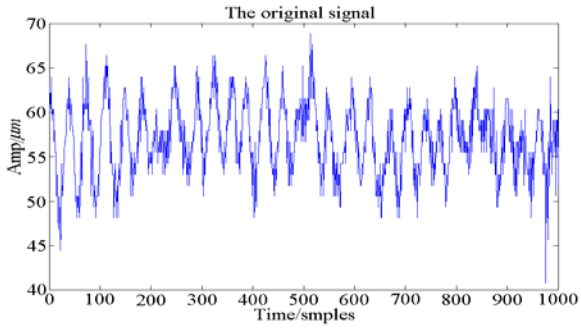

Fig .5 Oscillation signals of Hydroturbine

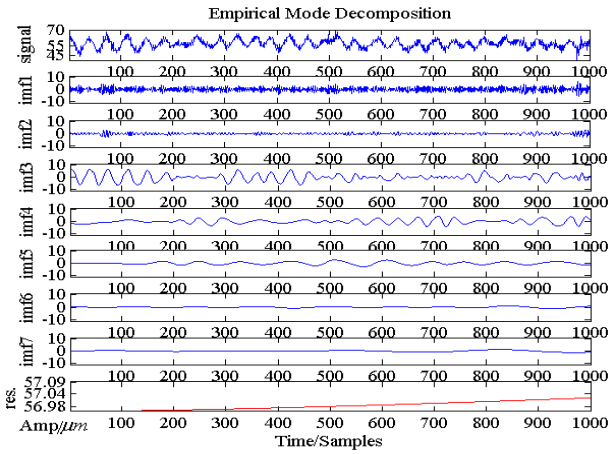

Fig.6 Empirical model decomposition

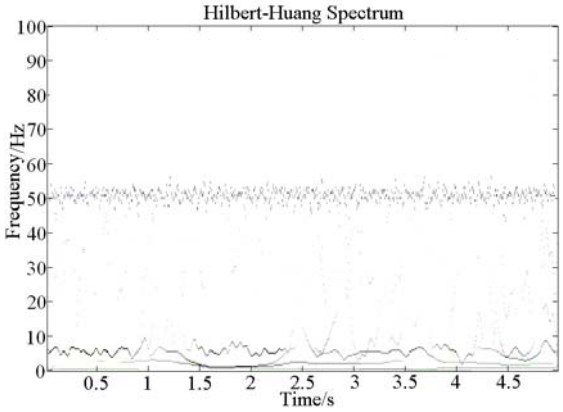

Fig .7 Original HHS

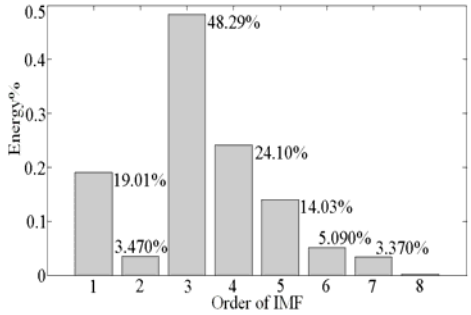

(a) Energy fluctuation ratio

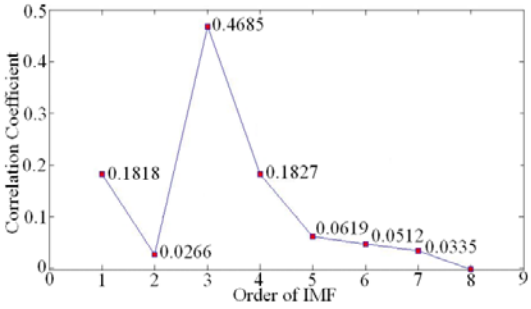

(b) Correlation fluctuation ratio

Fig.8 Energy-Correlation Fluctuation

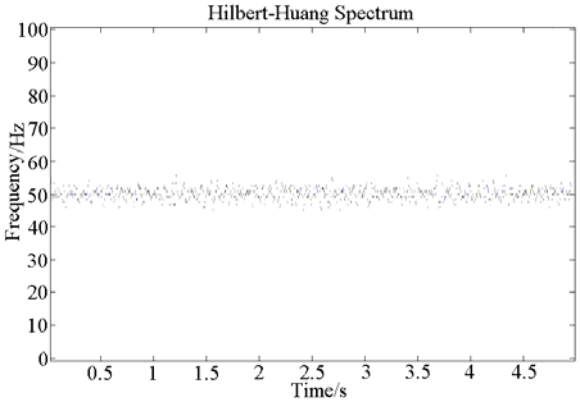

Fig .9 HHS of IMF1

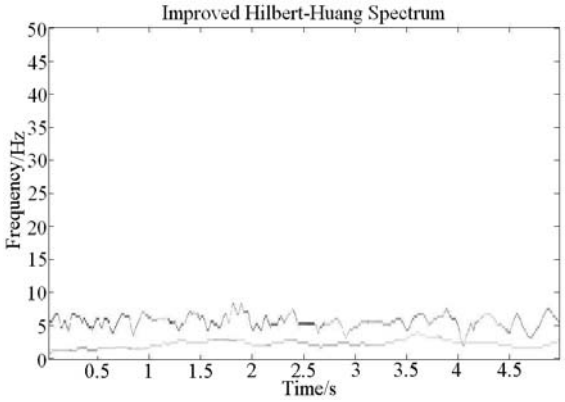

Fig .10 Improved HHS

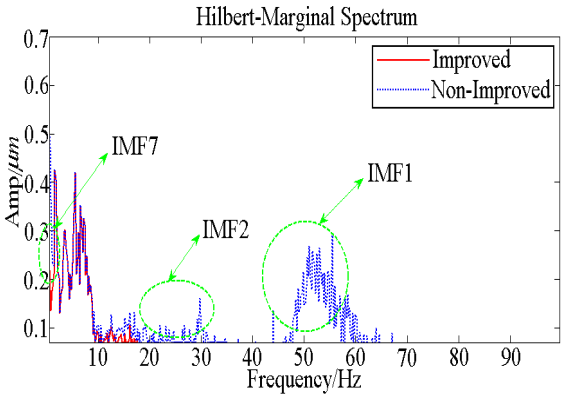

Fig .11 Boundary-Spectrum before and after improvement

Table .1 Parametric of Energy-Correlation

Energy	E_x	E_{x1}	E_{x2}	E_{imf1}	E_{imf2}	E_{imf3}	$E_{\cdot}$
	1.4700	0.9726	0.5000	0.9431	0.5082	0.0003	1.4516
Fluctuation		ε_1		ε_2		ε_3	
		0.6407		0.3453		0.0002	
		ρ_1		ρ_2		ρ_3	
		0.6504		0.3528		0.0003	
IO		Former		Improved		Elevation	
		0.0195		0.0128		24.1%	

Table .2 Parametric of Energy-Correlation

Energy	$E_{imf\,1}$	$E_{imf\,2}$	$E_{imf\,3}$	$E_{imf\,4}$	$E_{imf\,5}$	$E_{imf\,6}$	$E_{imf\,7}$
	0.3074	0.0561	0.7811	0.3898	0.2269	0.0824	0.0545
Fluctuation	ε_1	ε_2	ε_3	ε_4	ε_5	ε_6	ε_7
	0.1901	0.0347	0.4829	0.2410	0.1403	0.0509	0.0337
	ρ_1	ρ_2	ρ_3	ρ_4	ρ_5	ρ_6	ρ_7
	0.1818	0.0266	0.4685	0.1827	0.0619	0.0512	0.0335